CHAPTER 15

Empirical Modelling of Man-made Disaster Scenarios

Melanie Windirsch

Introduction

Natural catastrophes may make the headlines, but man-made perils can be equally destructive (Zurich Insurance Group 2017). In 2017, out of the 301 disaster events worldwide, 118 were man-made, resulting in USD 6 billion insured losses (Swiss Re Institute 2018c, pp. 2–4). Man-made disasters have the potential to jeopardise an individual insurer's solvency position if the risk is not properly managed. Furthermore, these catastrophes may trigger market shocks and subsequent economic downturns, like it happened in 2008s subprime financial crisis, because these events are highly destructive and result in the destruction of billions of physical property and infrastructure and affect millions of people and multiple

The views expressed in this paper are those of the author, and not necessarily those of Allianz.

M. Windirsch (✉)
Chicago, IL, USA
e-mail: melanie.windirsch@aol.com

T. Walker et al. (eds.), *Ecological, Societal, and Technological Risks and the Financial Sector*, Palgrave Studies in Sustainable Business In Association with Future Earth, https://doi.org/10.1007/978-3-030-38858-4_15

companies across different industries (e.g., banks, industrial companies). This kind of disaster leads to a disruption of business activities across regions (due to globalisation and high interconnectivity of business) and halts the economic output, taking several years to recover. These spill-over effects result in consequential amplifiers of this shock throughout the global economy and have an impact on both sides of an insurer's balance sheet—the losses that would be paid out in claims and the devaluation and reduction in returns in relation to the financial assets. Due to multiple insurers as well as other parties being affected by such market events, those losses may ultimately remove billions of anticipated Gross Domestic Product (GDP) from economies across the world (Cambridge Centre for Risk Studies 2018).

Due to an increase in frequency, duration, and magnitude of man-made disasters, the need for a comprehensive approach to identify, assess, transfer, and mitigate the risks arises today even more than in the past. Therefore, a proper estimation of their extent (frequency and severity) is important for the healthiness and future existence of insurance companies as well as the stability of the financial market.

Natural catastrophes are well understood. But unlike with natural hazards and their sophisticated risk models, the empirical modelling of man-made disaster scenarios is very challenging (Clark et al. 2015, p. 5-2) and mainly results from two facts:

1. Variety of loss triggers: The variety of loss triggers, such as explosions, collisions, human errors, leads to an even more unpredictable set of possible catastrophic risks.
2. Low frequency: It is often the case that sufficient historical claims data do not exist for man-made catastrophes (low frequency) to model those properly.

Nonetheless and especially because of their severity, there is a need to evaluate these risks, not only due to regulatory requirements, such as Solvency II, but also for internal purposes (e.g., planning or cost allocation) (Brüske et al. 2010, p. 134).

Due to the lack of empirical modelling approaches for man-made disaster scenarios, the insurance industry uses expert-based approaches to assess the frequency and severity of man-made catastrophes. In many cases, a group of experts estimates the frequency and severity of specific predefined scenarios based on experience. Combined with the potential loss

volume (derived from the analysis of internal portfolio data), an overall assessment of these scenarios can ultimately be conducted. Expert assessments are subjective views that result in relatively high uncertainties. This peculiarity is addressed as part of this research.

The ultimate goal of this research is to determine how the frequency and severity of tail events can be evaluated and modelled based on empirical data. Because of the variety of triggers that require separate modelling approaches, this research is focused on man-made fire/explosion disasters since recent events, such as the Tianjin harbor explosion,[1] have shown the significance of this disaster type and their impact on the insurance industry. Hence, empirical modelling shall be applied to develop a loss curve to ultimately reflect man-made fire/explosion disasters properly.

For this purpose, man-made disaster scenarios are defined and characterised first. Then, the main section focuses on the modelling of man-made disaster scenarios based on historical claims data. Once the data collection and preparation are explained, different methods for developing appropriate frequency and severity curves for man-made fire/explosion catastrophes are explored by fitting and validating different potential distributions. Ultimately, an aggregate loss distribution is derived, illustrating the probability for man-made fire/explosion catastrophes. A conclusion closes the research work.

Definition and Characteristics of Man-made Disasters and Their Distinction to Natural Hazards

Broadly, catastrophes (or so-called disasters/tail events) describe extremely negative but very rare events resulting in a sudden and massive destruction of property, lives, environment, and/or economy. Thus, disasters are characterised with high severity, but low frequency. They can either be caused by natural hazards or man-made events. Natural catastrophes refer to an event induced by natural forces (weather- or geological-related events) such as tropical cyclones, floods, tornadoes, hailstorms, wildfires,

[1] Tianjin harbor explosion is one of the largest global insurance losses in the history of man-made disasters. Current estimates assume insurance losses around USD 3.5 billion. In 2015, a hazardous chemical explosion occurred at a warehouse storing dangerous and flammable materials in the Port of Tianjin. The explosion caused enormous economic and human losses for enterprises and society. The review and analysis of the causes and effects of the explosion has triggered a wider discussion about risk management and the impact of man-made disasters (Swiss Re 2016, p. 1).

blizzards, earthquakes, tsunamis, volcanic eruptions, mudslides, or avalanches. Conversely, man-made catastrophes refer to accidental or intentional human actions. Hence, man-made disaster scenarios represent losses from single man-made catastrophic events that are deemed extreme and atypical but realistic (Banks 2009, pp. 17–22; Clark et al. 2015, p. 5-2).

Man-made disasters are characterised by various aspects that need to be taken into consideration (Thornton 2016, pp. 2–3):

- Variability: Man-made disasters can originate from various, very heterogeneous perils that show significant differing characteristics and treatment requirements. Hence, there is a broad variety of triggers.
- Geographical location: Some of the man-made disasters don't have geographical boundaries. Hence, accumulations cannot be defined in terms of the location of the insured parties, as for example in the case of cyberattacks.
- Sparse Data: Due to the low frequency of man-made disasters, there is limited historical data available used to perform risk assessments.
- Constant Evolution: Because of the nature of man-made disasters being affected by people and behaviour, they constantly evolve which deteriorates the data reliability topic as past performances cannot be used as a guarantee for future results.
- Prevention: Other than natural catastrophes, man-made disasters can theoretically be stopped or even prevented.

Man-made disaster scenarios can be divided into different clusters because they show similar characteristics. Cluster groups can mainly be structured according to the trigger that is causing a man-made disaster; for example, fire/explosion or collision (Lloyd's 2018). This contribution focuses on man-made fire/explosion disasters only as this particular man-made disaster cluster is of high importance, not only for insurance companies, but also for its significance and huge impact on the market.

Data Collection, Preparation, and Analysis

Data Collection and Preparation

Different external data sources that are used to build up a loss database for man-made fire/explosion disasters are first presented. To explicitly

capture man-made fire/explosion disasters, only the events that outline fire/explosion as triggers are considered for this exercise.

Reinsurance companies, acting as protectors for multiple insurance companies with regards to catastrophic risks, and similar reinsurance brokers, acting as intermediaries in this context, as well as marketplaces like Lloyd's, have access to a great variety of historical loss data due to their large portfolios. Therefore, the main reinsurance companies and brokers have been contacted to access their historical loss data for man-made fire/explosion disasters. In addition, the internet is screened for publicly available data on man-made catastrophes; a Google research is carried out to further identify large fire/explosion losses. For instance, Marsh regularly publishes an official report about the 100 largest property losses—current data is available for the time period 1974–2017 (Marsh 2016, 2018). Furthermore, Marsh also presents reports with information about historical loss experiences that have affected the power generation industry in recent years (Marsh 2014; Marsh 2012). Reuters, for example, provides an overview of the world's worst industrial accidents in the last 20 years (Cutler 2013). Additional insights are obtained through the list of historical explosions collected by the organisation Explosion Hazards Ltd. (ATEX Explosion Hazards Ltd. 2018). The database is built based on the various sources mentioned above.

Finally, it should be noted that it is quite challenging to access valuable data about historical fire/explosion catastrophe losses, especially for losses that occurred far in the past. Hence, it is almost impossible to build a complete database for large man-made fire/explosion losses worldwide. Nonetheless, the collected data as described above can be considered representative since various data sources are combined.

First, the historical losses that would no longer occur under current conditions, for example, due to a change in production mode, are removed from the list of historical industry loss data for man-made fire/explosion catastrophes.

Second, some events did not have the insured loss amount on record and only the total economic loss. Thus, the insured loss amount has to be derived thereof, since the total economic loss also includes the uninsured loss portion. To achieve this, the insured loss share of the total economic loss is to be identified by using the time-series comparison `Insured vs Uninsured Losses 1970–2016' from Swiss Re's sigma 1/2018 report as a basis (Swiss Re Institute 2018b). For every particular year, the insured loss share is calculated by dividing the man-made Insured Loss by the

man-made Total Economic Loss. Whereas the annual Insured Loss is specifically available for man-made catastrophes, the Total Economic Loss figure also includes Natural Catastrophes (NatCat). Hence, the annual Total Economic Loss for man-made catastrophes is to be calculated by deducting the NatCat portion from the overall figure. For the year 2001, the Insured Loss Share is calculated without consideration of the World Trade Center catastrophe as its inclusion would distort the results because of the extreme severity of this event. This calculation results in an average man-made Insured Loss Share of 63.14% for the time period 1970–2016. A correlation factor of 0.93 confirms the significance of the linkage between the Total Economic Loss and the Insured Loss per year. Depending on the event year, the respective Insured Loss Share for this particular year is to be multiplied with the Total Economic Loss figure to estimate the Insured Loss amount for the single event.

The collected historical loss data are further prepared to accurately reflect the changing environment. First, the inflation measured by the consumer price index (2010 base year) needs to be taken into account to adjust past loss amounts for the current living standards. Consumer Price Index (CPI) is defined as the period-to-period proportional change in the prices of a basket of goods and services that are purchased by the reference population (OECD 2019). As the CPI for USD is available for a longer time period, the adjustment for inflation is to be rendered in USD. Hence, the USD loss amount values are extrapolated using the US CPI to give the current (2017) values. The World Bank Group is used as a reasonable source for this purpose (The World Bank Group 2019). To adjust the losses per event for inflation, an individual inflation factor per event year is calculated by dividing the level of CPI 2017 by the level of CPI for the particular event year. To derive the adjusted loss values for inflation to 2017, the inflation factor is multiplied with the respective Gross Exposure value in USD (Swiss Re Institute 2018a).

In addition, different currencies also need to be converted to one central currency for further processing. All data available are converted into EUR by using a fixed exchange rate, that is 31.03.2018 (date of conversion) in this particular case.

Finally, all loss data from the different data sources are merged to a single overall fire/explosion loss database. To focus on catastrophic losses, all losses with a gross exposure/insured loss amount less than EUR 100 million (inflated amount) are removed and will no longer be considered for the following analysis.

Data Analysis

The overall man-made fire/explosion disaster loss database shows 114 fire/explosion losses with a gross exposure exceeding EUR 100 million for the time period 1974–2017.

Table 15.1 shows the major five man-made fire/explosion catastrophes.

The annual number of claims ranges from 0 to 7. The summarised measures for the 44-year sample of loss history of claim numbers are as follows (Gray and Pitts 2012, pp. 58–61):

mean 2.59, variance 3.83, standard deviation 1.96, min 0.00, max 7.00.

The average number of large fire/explosion losses is at 2.59 per year, but a negative trend can be observed, which predicts an average number of annual large fire/explosion losses between 3 and 4 at least for the next five years.

The size of claims ranges from EUR 101.29 million to EUR 2522.92 million. The summary measures per single event for the 44-year sample of loss history of claim sizes (in million EUR) are as follows (Gray and Pitts 2012, pp. 58–61):

mean 315.87, variance 111,624.8, standard deviation 334.10, min 101.29, max 2522.92.

The total loss amount for large fire/explosion losses for the time period 1974–2017 is roughly at EUR 36 billion. This leads to an average loss amount of EUR 316 million per event. The picture with regards to the annual loss amounts is very volatile with peaks in 1989 and 2011, which is illustrated in Fig. 15.1.

Large parts of the volatility can be explained by the differences regarding the number of events per year as the average loss amount per event is quite stable.

Table 15.1 Major five man-made fire/explosion catastrophes

Event year	*Location*	*Event*	*Gross insured loss in mn EUR*
2011	Cyprus	Vasilikos Power Station (Explosion)	2523
1988	North Sea	Piper Alpha (Fire/Explosion)	1433
1989	Texas	Polyolefin Plant Pasadena (Vapor Cloud Explosion)	1405
2017	Abu Dhabi	Ruwais Refinery (Fire)	1379
2015	Hertfortshire	Buncefield Oil Storage Depot (Fire)	1085

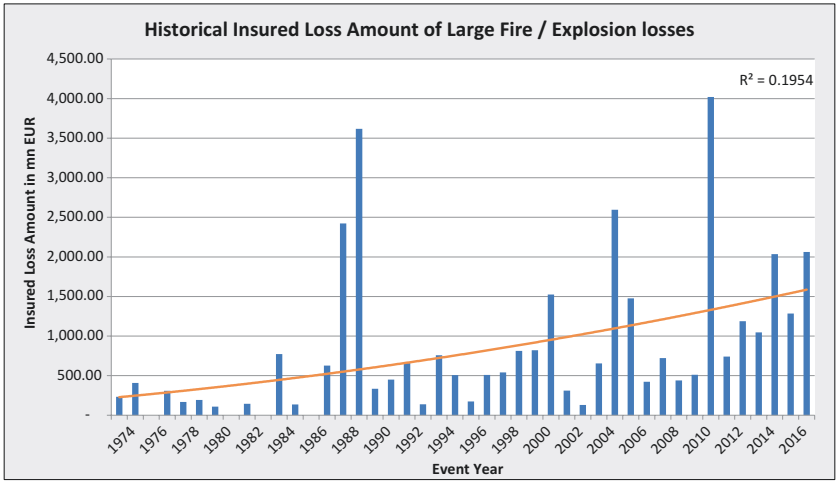

Fig. 15.1 Gross large fire/explosion loss amounts in mn EUR

The predicted future large fire/explosion loss amounts result in an average annual fire/explosion loss amount between EUR 1.5 billion and EUR 2 billion at least for the next five years. Linking these results to the predicted average number of events per year, an average loss amount of EUR 500 million per event may be assumed.

Overall a negative trend, in frequency and severity, is observable that shall be considered during the risk modelling process.

Developing a Loss Curve for Man-made Fire/Explosion Disasters based on Historical Industry Loss Data

Frequency Distribution

The **Poisson distribution** is the most commonly used distribution to model the frequency within a catastrophe model by giving the probability of a number of independent events occurring in a specific time frame (Mitchell-Wallace et al. 2017, p. 40; Wälder and Wälder 2017, p. 60). The Poisson family of distributions has a single parameter, called λ, which represents the mean of the distribution (Gray and Pitts 2012, p. 13).

The random variable X has a Poisson distribution $Pr(x)$ for $x = 0, 1, 2\ldots$ and parameter $\lambda > 0$, if the following applies (Forbes et al. 2011, pp. 152–156; Mitchell-Wallace et al. 2017, p. 40):

$$\Pr(x) = \frac{e^{-\lambda}\lambda^{x}}{x!} \tag{15.1}$$

$$E[X] = Var[X] = \lambda \tag{15.2}$$

The **negative binomial distribution** is used when a dependence between events is known. As in the case of this research, independence between the events of the underlying data set may be assumed due to the nature and type of the risk (man-made catastrophe), only the Poisson distribution shall be used for modelling the frequency (Mitchell-Wallace et al. 2017, p. 41).

To fit the Poisson distribution $Poi(\lambda)$, parameter λ is to be estimated first. For this purpose, the claims data for the time period 1974–2017 is classified according to the number of claims per year exceeding the threshold of EUR 100 million. This is illustrated in Table 15.2.

Independent whether the Method of Moments or the Method of Maximum Likelihood is used, parameter λ can be derived by calculating the sample mean $E[X]$ from the existing data set. The calculation can be summarised as follows:

$$\text{Sample Mean} = E[X] = \bar{x} = \frac{1}{44}\sum_{j=0}^{7} r\, f_r = 2.5909 = \lambda$$

Table 15.2 Number of claims per year

Number of claims per year r	*Frequency (number of years affected)* f_r
0	4
1	13
2	8
3	6
4	5
5	3
6	3
7	2
>7	0

The fitted distribution is then calculated using the fitted frequency for r claims, $\hat{f}_r = 44 * \Pr(X = r)$, where $X \sim Poi(2.5909)$. Hence, the fitted claims frequency is calculated by applying $\hat{f}_r = 44 * \Pr(x) = 44 * \frac{e^{-2.5909} 2.5909^x}{x!}$ to the respective annual number of claims (Gray and Pitts 2012, pp. 60–61).

Table 15.3 compares the observed with the fitted claims frequency for the 44-year sample period.

Based on the elaboration above, the following frequency distribution is used to describe the annual number of claims exceeding EUR 100 million:

$$\Pr(x) = \frac{e^{-2.5909} 2.5909^x}{x!}$$

This is ultimately resulting in the graph as per Fig. 15.2.

Now, the goodness of fit of this distribution is assessed by using informative visual displays and appropriate test statistics to evaluate the adequacy of the Poisson distribution.

A visual inspection is used to evaluate the quality of the frequency distribution (Forbes et al. 2011, pp. 69–73). For this purpose, the observed and expected frequency values are compared in Fig. 15.3.

The graph shows a quite harmonised course of both curves, even though the peak for the observed frequency curve is at one claim per year, while the fitted frequency has its peak at two claims per year. In addition, the upper tail of the observed frequency is heavier than the fitted frequency tail. Nonetheless, the flow of both curves overall fits. Hence from a visualisation point of view, the fitted frequency may be deemed appropriate.

Table 15.3 Observed versus fitted (Poisson distribution) frequency of claims

Number of claims	*Observed frequency*	*Poisson fitted claims frequency*
0	4	3.2979
1	13	8.5445
2	8	11.0690
3	6	9.5596
4	5	6.1920
5	3	3.2086
6	3	1.3855
7	2	0.5128
>7	0	0.0

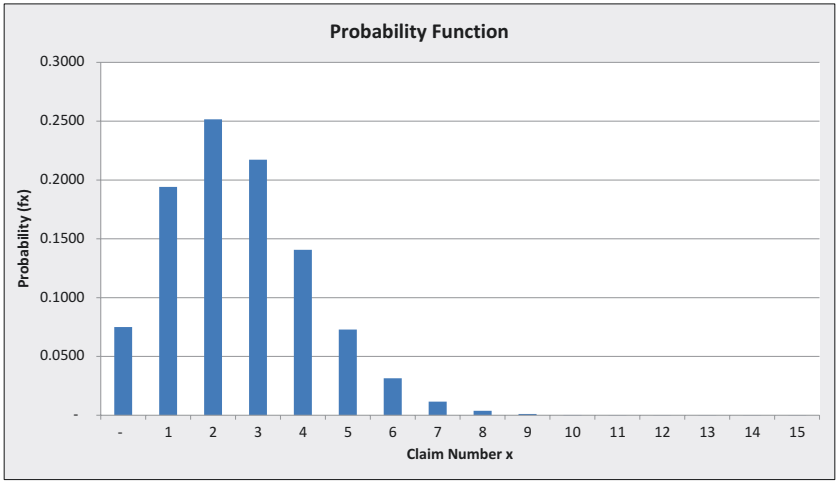

Fig. 15.2 Claim number probability function (Poisson distribution)

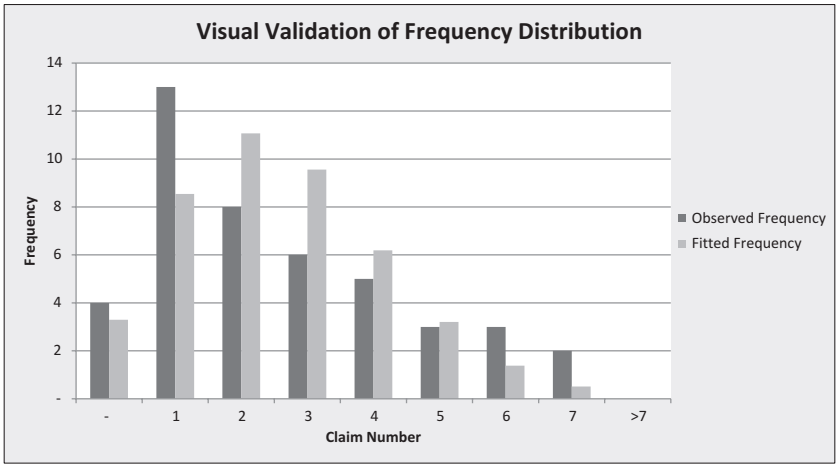

Fig. 15.3 Visualisation observed versus fitted frequency

As a second and even more important approach, an appropriate test statistic is used to evaluate the quality of the frequency distribution. To perform the Pearson chi-square goodness-of-fit test, the null hypothesis regarding the frequency distribution is to be formulated first (Forbes et al. 2011, pp. 69–73):

There is no significant difference between the observed and the expected values with respect to the number of claims per year exceeding EUR 100 million.

To fulfil the minimum requirements in terms of fitted frequency,[2] the cells for six and seven claims per year need to be combined as the expected frequency for seven or more losses per year does not exceed the value of 1 (Gray and Pitts 2012, pp. 63–65). This combination leads to the results in Table 15.4 that can now be used to perform the Pearson chi-square goodness-of-fit test.

As one parameter is estimated in the fitting process of the Poisson distribution and as seven cells are used during calculation, the appropriate chi-squared distribution has parameter $a = 5$, degrees of freedom. Applying the outlined formula, the calculation looks as follows:

$$X^2 = \sum \frac{(O - E)^2}{E} = 9.9598$$

This results in a p-value of 0.0764. As this value exceeds the significance level of 0.05, the Poisson distribution may be deemed appropriate to reflect the claim size of the existing data set (GraphPad Software 2019).

Furthermore, comparing the calculated X^2 value with the table value of the chi-squared distribution, that is, 11.07 for $a = 5$ degrees of freedom and a confidence level of 95%, results in the conclusion that the null hypothesis is accepted, as the calculated value is less than the table value.

Table 15.4 Observed frequency versus adjusted fitted claims frequency

Number of claims	*Observed frequency*	*Poisson fitted claims frequency*
0	4	3.2979
1	13	8.5445
2	8	11.0690
3	6	9.5596
4	5	6.1920
5	3	3.2086
≥6	5	1.8984

[2] A cell is only deemed usable if the expected frequency is not too small, meaning all cells need to reach $E \geq 1$, and not more than 20% of the cells should have $E < 5$. If the frequencies are too low, neighbouring cells are combined.

Therefore, it can be concluded that there is no significant difference between the observed and expected values.

To summarise, it can be observed empirically that the fit of the Poisson distribution is considered good as the frequencies expected under the fitted model are not far away from the observed frequencies; in particular, the Poisson model is also capable of reproducing the tail of the observed data. The observed data shows 5 out of 44 years with six or more large fire/explosion losses exceeding EUR 100 million, while the Poisson fit manages an expected frequency of about 1.9—the tail of the fitted Poisson is slightly too light but still appropriate. Since the Poisson distribution is a member of a single-parameter family, its distribution is not very flexible, and its ability to fit an observed frequency distribution is restricted. Nevertheless for this purpose, the selected distribution seems to reflect the data set accordingly. Formally, the hypothesis that the number of claims follows a Poisson distribution is confirmed (Gray and Pitts 2012, pp. 63–65).

Severity Distribution

With respect to modelling the severity, Pareto, Weibull, or lognormal distributions are often used (Embrechts and Schmidli 1994, pp. 7–10).

To identify which of these distributions are worth modelling, the mean-excess function is considered because it describes the distribution in the tail quite good. As the area around the large quantiles is extremely risk relevant, it is important to determine a distribution that is close to the empirical distribution in this area. The mean excess function $e(t)$ of a random variable X with $X \geq 0$ describes the expected exceedance of a given threshold and is defined as follows:

$$e(u) := E\left(X - u | X > u\right) = \frac{\int_u^\infty (t-u) f(t)\, dt}{P(X > u)}$$

For the empirical case with $x_1, \leq \ldots \leq x_n$ large losses, the following applies:

$$e_n(u) = \frac{\sum_{i=1}^n x_i \big|_{x_i} > u}{\sum_{i=1}^n \big| x_i > u} - u$$

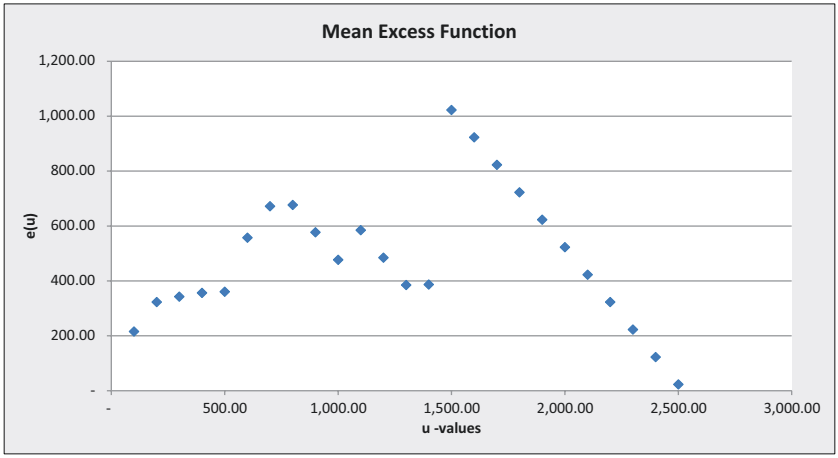

Fig. 15.4 Mean excess function (empirical data)

with $\mathbb{1}_{x>u}$ being the indicator function that equals the value 1 for $x > u$ and 0 in any other case (Brüske et al. 2010, pp. 137–138; Embrechts et al. 2003, pp. 294–297; Embrechts and Schmidli 1994, p. 11).

For the existing data set, the mean excess function for different thresholds t results in the graph as per Fig. 15.4.

Comparing this figure to the graphs of the mean excess function $e(u)$ of some standard distributions indicates that all distributions as outlined above might potentially be capable of reflecting the empirical data accordingly.

First, the Pareto distribution will be considered, including two types: the one parameter Pareto and the three parameter Generalized Pareto distribution.

Due to their characterisation as heavy-tailed distributions, **Pareto distributions** are appropriate for modelling the severity of catastrophe losses (Brüske et al. 2010, pp. 137–138; Wälder and Wälder 2017, pp. 51–52). There are different types of Pareto distributions. The **one parameter Pareto distribution** is often used in catastrophe pricing. In general, the distribution has two parameters, although one is not a free parameter as it is defined upfront by the threshold t beyond which the distribution applies. For threshold >0, $x > t$ and parameter $a > 0$, the one parameter Pareto distribution is given as follows:

$$f(x) = \frac{at^a}{x^{a+1}}$$

$$F(x) = 1 - \left(\frac{t}{x}\right)^a$$

$$E[X] = \frac{at}{a-1}$$

$$\mathrm{Var}[X] = \frac{at^2}{(a-1)^2(a-2)}$$

If the mean can be calculated based on the existing data set, parameter a is estimated using the following formula (Forbes et al. 2011, pp. 149–151; Mitchell-Wallace et al. 2017, p. 43):

$$a = \frac{E[X]}{E[X] - t}$$

To fit the **one parameter Pareto distribution** $Par(a, t)$, threshold t and parameter a are to be defined. Threshold t reflects the amount beyond which the distribution applies. As the existing data set only considers losses exceeding EUR 100 million, threshold t is defined as $t = 100$. To finally fit the one parameter Pareto distribution, parameter a is estimated. For this purpose, the sample mean is calculated as follows:

$$\text{Sample Mean} = E[X] = \bar{x} = \frac{1}{114}\sum_{n=1}^{114} X_n = 315.87$$

Based on the sample mean $E[X] = 315.87$ and threshold $t = 100$, parameter a is calculated as follows:

$$a = \frac{E[X]}{E[X] - t} = \frac{315.87}{315.87 - 100} = 1.4632$$

Applying the parameter as defined above, the following severity distribution is used to describe the claim size exceeding EUR 100 million:

$$f(x) = \frac{1.4632 * 100^{1.4632}}{x^{2.4632}}$$

The cumulative distribution function is then determined as follows (Forbes et al. 2011, pp. 149–151; Mitchell-Wallace et al. 2017, p. 43):

$$F(x) = 1 - \left(\frac{100}{x}\right)^{1.4632}$$

This is ultimately resulting in the graphs as per Figs. 15.5 and 15.6.

To model a specific claim size section beyond a particular threshold, the **three parameter Generalized Pareto distribution** is commonly considered (Peng and Welsh 2001, pp. 53–54). For parameters k (shape parameter) with $k \in R$, σ (scale parameter) with $\sigma > 0$, and ξ (location parameter) with $\xi \in R$, the Generalized Pareto distribution is given as follows (Zea Bermudez and Kotz 2010, p. 1354):

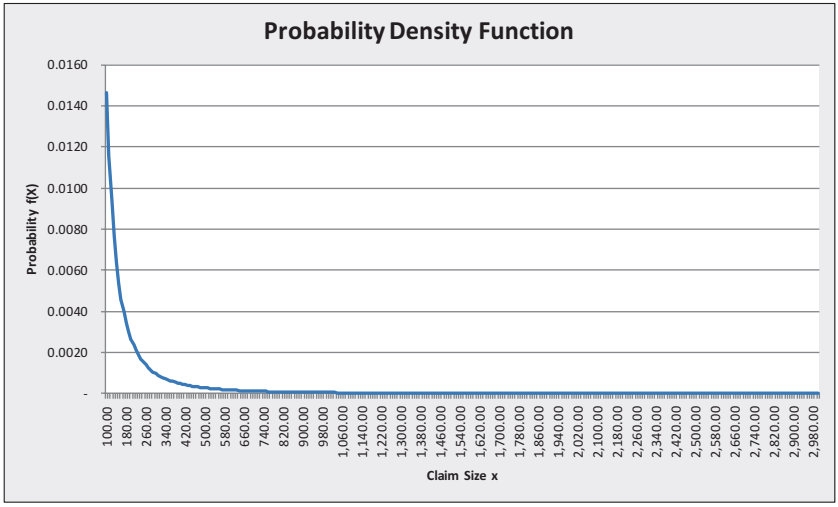

Fig. 15.5 Claim size probability density function (one parameter Pareto distribution)

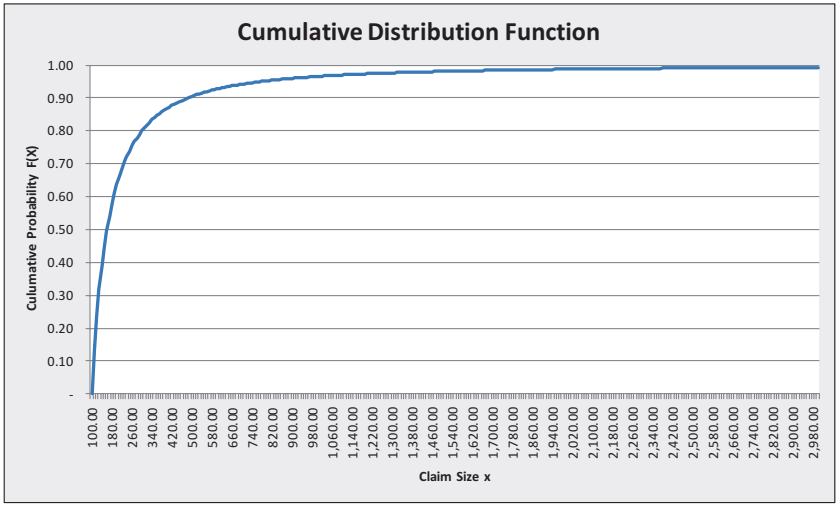

Fig. 15.6 Claim size cumulative distribution function (one parameter Pareto distribution)

$$f(x) = \begin{cases} \frac{1}{\sigma}\left(1 - k\frac{x-\xi}{\sigma}\right)^{\frac{1}{k}} & for\ k \neq 0 \\ \frac{1}{\sigma} e - \frac{x-\xi}{\sigma} & for\ k = 0 \end{cases}$$

$$F(x) = \begin{cases} 1 - \left[1 - \frac{k}{\sigma}(x-\xi)\right]^{\frac{1}{k}} & for\ k \neq 0 \\ 1 - e - \frac{x-\xi}{\sigma} & for\ k = 0 \end{cases}$$

To fit the **three parameter Generalized Pareto distribution** (k, ξ, σ), parameters k, ξ and σ are to be defined first. Several methods exist in literature to estimate these parameters, but the Method of Maximum Likelihood is mostly used (Zea Bermudez and Kotz 2010, p. 1354). One of the major prerequisites to achieve reliable results through its application is a minimum size sample of 500 data points. For smaller samples (like in the case of this research), estimators derived from the Method of Moments are

more reliable (Zea Zea Bermudez and Kotz 2010, p. 1354). The Method of Moments of parameters k, ξ, and σ can be derived by solving the related equations for the moment estimators (Hosking and Wallis 1987, p. 341; Singh and Guo 1995, p. 174):

First, the moment estimates of k is obtained by determining the sample skewness and solving the third equation (Hosking and Wallis 1987, p. 341):

$$\hat{k} = \frac{1}{2}\left(\frac{\bar{x}^2}{s^2 - 1}\right) = 0.4469$$

Using parameter $k = 0.4469$, parameter σ can be calculated by solving the second equation (Singh and Guo 1995, p. 174):

$$\sigma = S(1+k)(1+2k)^{0.5} = 665.2683$$

Using parameters $k = 0.4469$ and $\sigma = 665.2683$, parameter ξ can be calculated by solving the third equation:

$$\xi = \bar{x} - \frac{\sigma}{\sigma + k} = 314.8708$$

Applying the parameters defined above, the following severity distribution may be used to describe the claim size exceeding EUR 100 million (as $k \neq 0$ applies) (Zea Bermudez and Kotz 2010, p. 1354):

$$f(x) = \frac{1}{665.2683}\left(1 - 0.4469\frac{x - 314.8708}{665.2683}\right)^{\frac{1}{0.4469}}$$

The cumulative distribution function is then determined as follows (as $k \neq 0$ applies):

$$F(x) = 1 - \left[1 - \frac{0.4469}{665.2683}(x - 314.8708)\right]^{\frac{1}{0.4469}}$$

As for catastrophic risks, extreme value distributions are often used and thus the **Weibull distribution** is next considered. The random variable X has a Weibull distribution for $0 \leq x < \infty$ and parameters $a > 0$ and $\beta > 0$, if the following applies (Forbes et al. 2011, pp. 193–201):

$$f(x) = \frac{\beta x^{\beta-1}}{a^{\beta}} e - \left(\frac{x}{a}\right)^{\beta}$$

$$F(x) = 1 - e - \left(\frac{x}{a}\right)^{\beta}$$

$$E[X] = a\Gamma\left(\frac{\beta+1}{\beta}\right)$$

$$\mathrm{Var}[X] = a^2\Gamma\left(\frac{\beta+2}{\beta}\right) - \left[\Gamma\left(\frac{\beta+2}{\beta}\right)\right]^2$$

To fit the **Weibull distribution** $Wei(a, \beta)$, parameters a (shape parameter) and β (scale parameter) are to be defined first. Applying the Method of Maximum Likelihood requires the application of a numerical method as both parameters are unknown (Gray and Pitts 2012, p. 60). The log-likelihood function is given by:

$$l_n(a,\beta) = n\log a - n\log\beta + (a-1)\Sigma\log\left(\frac{x_i}{\beta}\right)\Sigma\left(\frac{x_i}{\beta}\right)^a$$

To maximise the log-likelihood function, an iterative procedure is used. The Newton-Raphson method is one common option to be applied (Nwobi and Ugomma 2014, p. 69; Pobočíková and Sedliačková 2014, p. 4141). The method starts with a function h defined over the sample data set n with values x_i, the function's derivative h' and an initial guess β_0 for the value of β. To define a new estimate for the value of β, i.e. β_{k+1}, the following calculation is performed:

$$\beta_{k+1} = 1 - \frac{h(\beta_k)}{h'(\beta_k)} \text{ with } h(\beta) = \frac{1}{\beta} + \frac{u}{n} - \frac{w}{v} \text{ and } h'(\beta) = -\frac{1}{\beta^2} + \frac{w^2}{v^2} - \frac{s}{v},$$

The calculation is repeated until the value of β_k converges, meaning that $h(\beta_k)$ becomes close to zero. Based on parameter $\hat{\beta}$, parameter $\hat{\alpha}$ can be calculated using the following formula (Zaiontz 2019):

$$a = \left(\frac{v}{n}\right)^{\frac{1}{\beta}}$$

Applying the described methodology to the underlying data set results in the following parameter estimates:

$$\hat{a} = 342.3824$$
$$\hat{\beta} = 1.2269$$

Applying the parameter as defined above, the following severity distribution may be used to describe the claim size exceeding EUR 100 million (Forbes et al. 2011, pp. 193–201):

$$f(x) = \frac{1.2269x^{0.2269}}{342.3824^{1.2269}} e - \left(\frac{x}{342.3824}\right)^{1.2269}$$

The cumulative distribution function is then determined as follows:

$$F(x) = 1 - e - \left(\frac{x}{342.3824}\right)^{1.2269}$$

ultimately resulting in the graphs as per Figs. 15.7 and 15.8.

Conditional distributions may be considered to model the probability of a claim size exceeding a particular threshold. For this purpose, the **lognormal distribution** is considered to reflect the conditional tail probability. The random variable X has a lognormal distribution for $x > 0$ and the two parameters, μ and σ, if the following applies (Gray and Pitts 2012, pp. 23–36; Wälder and Wälder 2017, p. 50):

$$f(x) = \frac{1}{\sigma\sqrt{2\pi}} \frac{1}{x} e^{-\frac{1}{2}\left(\frac{\log x - \mu}{\sigma}\right)^2}$$

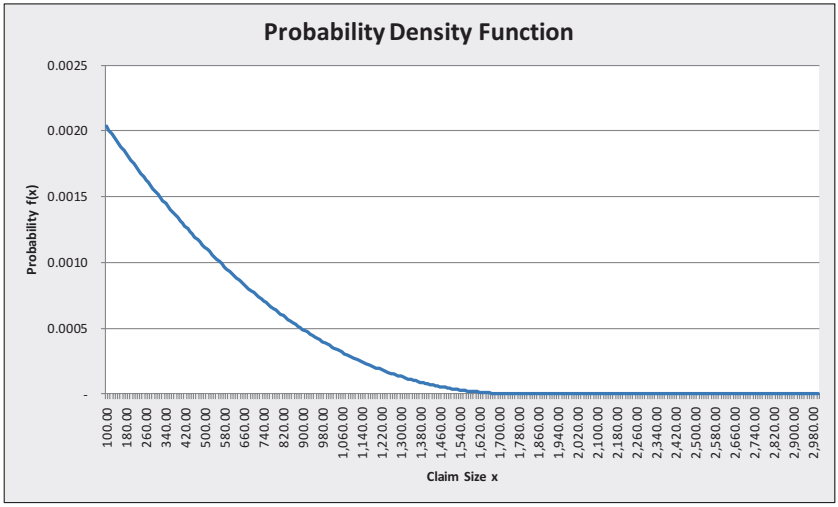

Fig. 15.7 Claim size probability (Weibull distribution)

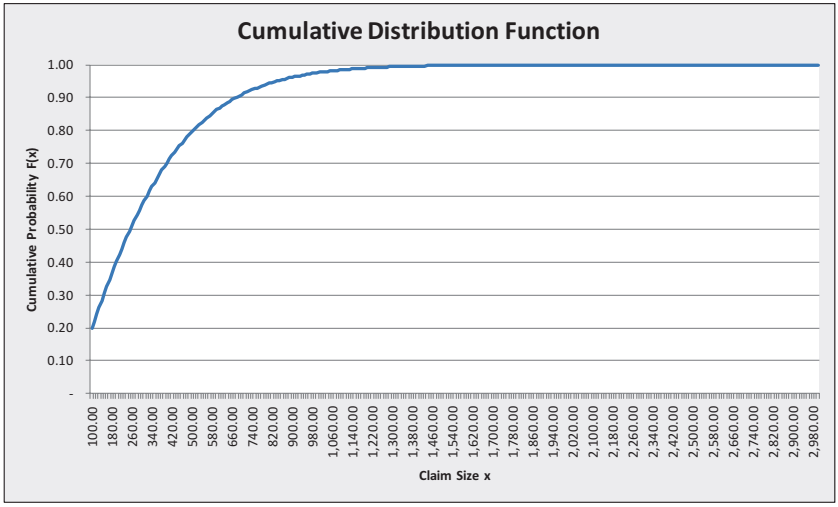

Fig. 15.8 Claim size cumulative distribution function (Weibull distribution)

(1) $F(x) = \Pr\left(Z < \dfrac{\log x - \mu}{\sigma}\right)$, the distribution function is determined by using the log transformation to normal and the distribution function of the standard normal distribution $Z \sim N(0, 1)$.

$$E[X] = e^{\mu + \frac{1}{2}\sigma^2}$$

$$\mathrm{Var}[X] = e^{\left(2\mu + \sigma^2\right)\left(e^{\sigma^2} - 1\right)}$$

To fit the **lognormal distribution** *lognormal*(μ, σ), parameters μ and σ are to be defined first. Applying the Method of Maximum Likelihood (MLE), the MLEs of μ and σ can be derived from the logged data as the sample mean and standard deviation of the log(x_i) values. Their calculations can be summarised as follows (Gray and Pitts 2012, p. 36):

$$\hat{\mu} = \overline{y} = \overline{\log x_i} = \frac{1}{114}\sum_{n=1}^{114} \log x_i = 2.3747$$

$$\hat{\sigma} = \left(\frac{1}{114}\sum_{114}^{i=1}\left(y_i - \overline{y}\right)^2\right)^{\frac{1}{2}} = 0.2941$$

Applying the parameter as defined above, the following severity distribution may be used to describe the claim size exceeding EUR 100 million:

$$f(x) = \frac{1}{0.2941\sqrt{2\pi}}\frac{1}{x}e - \frac{1}{2}\left(\frac{\log x - 2.3747}{0.2941}\right)^2$$

The cumulative distribution function is then determined by using the log transformation to normal and the distribution function of the standard normal distribution $Z \sim N(0, 1)$:

$$F(x) = \Pr\left(Z < \frac{\log x - 2.3747}{0.2941}\right)$$

Although the normal, exponential, and gamma distributions are widely used to model the severity of insurance losses, they will not be considered due to their thin-tailed characteristics.

Now, the goodness of fit of these distributions is assessed by using informative visual displays and appropriate test statistics to finally decide which distributions are selected for further processing.

A visual inspection is first used to evaluate the quality by comparing the empirical cumulative distribution function with the various fitted cumulative distribution functions. For independent and identically distributed random variables X_1, X_2, …, X_n the empirical cumulative distribution function is defined as

$$F_n(x) = \frac{1}{n}\sum_{i=1}^{n} \mathbb{1}(X_i \le x)$$

with $\mathbb{1}(X_i \le x)$ being the indicator function that equals the value 1 for $X_i \le x$ and 0 in any other case (Gray and Pitts 2012, pp. 63–65). The result is shown in Fig. 15.9.

The graph shows a quite harmonised course of the empirical cumulative distribution function and the **one parameter Pareto distribution**

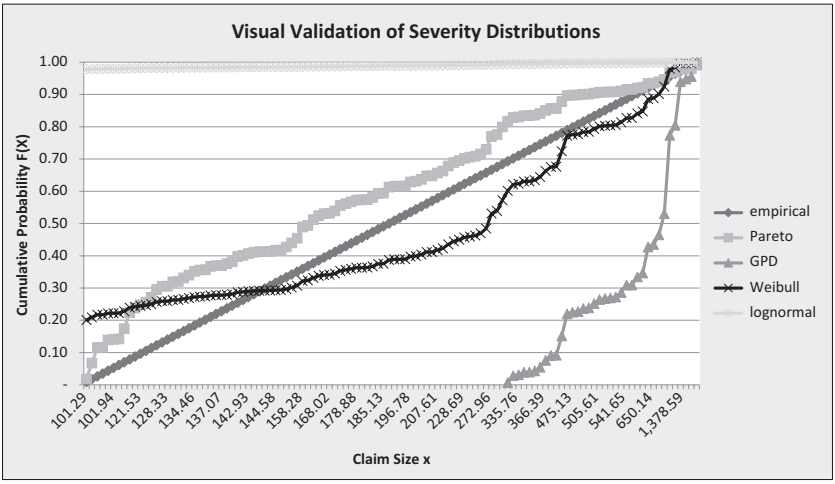

Fig. 15.9 Visualisation empirical versus fitted distribution functions

function; however, the **Weibull distribution** function seems to be quite adequate too, even though it seems to overemphasise the lower tail. The graph already outlines that the **Generalized Pareto** and the **lognormal distribution** do not reflect the empirical data at all. From a visualisation point of view, the one parameter Pareto distribution may be deemed the most appropriate one, but as this is not completely clear, further tests are carried out.

Therefore, as a second and even more important approach, an appropriate test statistic is used to evaluate the quality of the severity distributions. To perform the Pearson chi-square goodness-of-fit test, the null hypothesis regarding the severity distribution is to be formulated first (Forbes et al. 2011, pp. 69–73):

> *There is no significant difference between the observed and the expected values with respect to the size of a single claim exceeding EUR 100 million.*

The chi-squared test divides the observed claim sizes into k intervals and compares the observed counts (number of data values observed in interval i) to the number expected given the fitted distribution (number of data values expected in interval i) (Packová and Brebera 2015, p. 18). To fulfil the minimum requirements in terms of fitted frequency,[3] the observed claim sizes need to be combined to specific categories (Gray and Pitts 2012, pp. 63–65).

The results are shown in Table 15.5 that now can be used to perform the Pearson chi-square goodness-of-fit test.

Already at a first glance (and hence similar to the visualisation test), it is obvious that only two distribution functions have the potential to pass the goodness-of-fit test. The Generalized Pareto Distribution fails completely in the lower tail (no claims expected for loss volumes lower than EUR 300 million, even though the observed data show a major frequency in this area) and overemphasises the upper tail with a huge frequency for claims with loss volumes greater than EUR 1 billion. The lognormal distribution behaves even worse as it only covers claims with loss volumes in the area between EUR 100 million and EUR 150 million.

[3] A cell is only deemed usable if the expected frequency is not too small, meaning all cells need to reach $E \geq 1$, and not more than 20% of the cells should have $E < 5$. If the frequencies are too low, neighbouring cells are combined.

Table 15.5 Observed versus expected frequency for different claim size categories

Claims interval	*Observed frequency*	*Expected frequency Pareto*	*Expected frequency GPD*	*Expected frequency Weibull*	*Expected frequency Lognormal*
100–150	39	51.0145		34.7268	112.3157
150–200	24	21.6403		11.2988	0.4650
200–250	12	11.5173		10.2141	0.2794
250–300	3	6.9845		9.0512	0.1848
300–350	6	4.6128	5.9320	7.9029	0.1304
350–400	4	3.2357	8.1419	6.8200	0.0964
400–450	1	2.3739	7.7907	5.8291	0.0737
450–500	6	1.8032	7.4425	4.9413	0.0580
500–750	8	4.8410	32.1014	14.8917	0.1662
750–1000	0	2.0535	23.9067	5.5745	0.0764
1000–1250	2	1.0929	16.2274	1.8987	0.0424
>1250	4	2.8305	12.4575	0.8509	0.1115

Therefore, only the one parameter Pareto as well as the Weibull distribution function will be considered for further analysis.

As for the one parameter Pareto distribution, only one parameter is estimated in the fitting process, and 12 categories are used during calculation, the appropriate chi-squared distribution has parameter $a = 10$ degrees of freedom. Applying the above outlined formula, the calculation looks as follows:

$$X^2 = \sum \frac{(O - E)^2}{E} = 33.5817$$

This formula results in a p-value of 0.0002. As this value by far falls below the significance level of 0.05, the one parameter Pareto distribution may not be deemed appropriate to reflect the claim size of the existing data set (GraphPad Software 2019).

Furthermore, comparing the calculated X^2 value with the table value of the chi-squared distribution, that is 3.940 for $a = 10$ degrees of freedom and a confidence level of 95%, results in the conclusion that the null hypothesis is denied, as the calculated value is higher than the table value. Hence, it can be concluded that there is a significant difference between the observed and expected values.

As for the Weibull distribution, two parameters are estimated in the fitting process and 12 categories are used during calculation, the appropriate chi-squared distribution has parameter $a = 9$ degrees of freedom. Applying the outlined formula, the calculation looks as follows:

$$X^2 = \sum \frac{(O - E)^2}{E} = 42.4882$$

This formula results in a p-value of 0.0001. As this value by far falls below the significance level of 0.05, the Weibull distribution may not be deemed appropriate to reflect the claim size of the existing data set (GraphPad Software 2019).

Furthermore, comparing the calculated X^2 value with the table value of the chi-squared distribution, that is 3.325 for $a = 9$ degrees of freedom and a confidence level of 95%, results in the conclusion that the null hypothesis is denied, as the calculated value is higher than the table value. Hence, it can be concluded that there is an extremely significant difference between the observed and expected value.

To summarise, it can be observed empirically that the fit of none of the reviewed severity distributions is good because the expected frequencies for particular claim size intervals under the fitted model in some parts are far away from the observed frequencies; in particular, these distributions are not capable of reproducing the tail of the observed data. Formally, the hypotheses that the size of claims has a one parameter Pareto or Generalized Pareto or Weibull or lognormal distribution is to be denied. The conclusion is that none of these distributions provides an adequate description of the variation in the claim sizes that has been observed.

Even though none of the distribution properly fits, the one parameter Pareto distribution, providing the best fit, will be considered going forward to allow the development of an approximation of the aggregate loss distribution for large fire/explosion catastrophes.

Aggregate Loss Distribution

The aggregate loss distribution is determined by the frequency and severity distribution and describes the probability of the annual expected total loss resulting from large fire/explosion losses with individual loss volumes exceeding EUR 100 million (Cottin and Döhler 2013, p. 27). Both

distributions have been modelled on an individual basis and now need to be combined through an approximation method (Gondring 2015, p. 539). As both, claim size and claim number, are random variables expressed by a distribution, the collective model of risk aggregation is to be applied (Cottin and Döhler 2013, pp. 88–92). For the following, it is worth highlighting that claim size and claim number will be deemed independent. For the purpose of aggregation, compound distributions may be considered. For a known claim number distribution function $p_N(t)$ and a known claim size distribution function $F(x)$, the aggregate loss distribution is given as:

$$G(x,t) = p_0(t) + \sum_{\infty}^{v=1} p_v(t) * F^{*v}(x)$$

with $F^{*v}(x)$ being the v-fold convolution of the distribution function $F(x)$ that is calculated as follows:

$$F^{*1}(x) = F(x),\ F^{*k}(x) = \left(F^{*(k-1)} * F\right)(x) \text{ for } K > 1$$

Determining the aggregate loss distribution is quite challenging as the simplified approximation method via Panjer recursion cannot be used: The main prerequisite that the claim size X can only have values 0, h, $2h$, $3h$, …, does not apply for the existing data set. This challenge can only be solved with the support of statistical applications, such as Matlab or Solver. Using the command 'PsiPareto(1.4632, 100, PsiCompound(PsiPoisson(2.5909)))' the graphs of the aggregate loss distribution can be derived.

Because an explicit calculation of the aggregate loss distribution is not available for the distributions used, Monte Carlo simulation is an acceptable alternative to derive the aggregate loss distribution (Betram and Feilmeier. 1987; Mikosch 2009). For this, a series of incidental claim numbers N_1, N_2, N_3, … is to be created based on the predefined claim number distribution, that is, $\Pr(x) = \frac{e^{-2.5909}2.5909^x}{x!}$. Then, for every claim number $N_i (i = 1, 2, 3\ldots)$, a series of incidental claim size values $X_1^{(i)}, X_2^{(i)}, X_3^{(i)}, \ldots$ is to be assigned based on the predefined claim size distribution, that is, $F(x) = 1 - \left(\frac{100}{x}\right)^{1.4632}$.

For every $i = 1, 2, \ldots, n$ the annual aggregate loss $S^{(i)}$ is calculated as follows:

$$S^{(i)} = \sum_{j}^{N_i} X_j^{(i)}$$

This formula results in the following aggregate loss distribution function:

$F_s(x) \approx \frac{m(x)}{n}$ with $m(x)$ being the number of all $S^{(i)}$.

If simulating in Excel, the inverse of the respective cumulative distribution functions is to be determined to define the incidental values for both, claim number and claim size. Based on the simulated annual aggregate losses, the aggregate loss distribution can be derived through applying the fitting process. Due to the permanent changing values in Excel, only a snapshot can be discussed in the following by using the particular values from one simulation cycle as a basis to fit the distribution (Wälder and Wälder 2017, pp. 83–85). Due to limited computer capacity, a simulated sample of size 1000 is considered appropriate. When analysing the simulated data, it is quite obvious that the Exponential distribution might be a good fit.

To fit the **Exponential distribution** $Exp(\lambda)$, parameter λ is estimated. For this, the sample mean is calculated (Gray and Pitts 2012, pp. 25–26). The calculation can be summarised as follows:

$$\text{Sample Mean} = E[X] = \bar{x} = \frac{1}{1000}\sum_{n=1}^{1000} X_n = 787.2676$$

Based on the sample mean $E[X] = 787.2676$ parameter, λ can be calculated as follows:

$$\lambda = \frac{1}{E[X]} = \frac{1}{787.2676} = 0.0013$$

Applying the parameter as defined above, the following aggregate loss distribution is used to describe the annual aggregated loss volume for large fire/explosion losses exceeding EUR 100 million:

$$f(x) = \lambda e^{-\lambda x} = 0.0013 e^{-0.0013x}$$

The cumulative distribution function for $x > 0$ is then determined as follows:

$$F(x) = 1 - e^{-\lambda x} = 1 - e^{-0.0013x}$$

This formula is ultimately resulting in the graphs as per Figs. 15.10 and 15.11.

To confirm the validation of the developed aggregate loss distribution, a visual inspection is used by comparing the empirical with the fitted cumulative distribution function (Gray and Pitts 2012, pp. 65–67). The results are shown in Fig. 15.12.

The graph shows a quite harmonised course of the empirical cumulative distribution function and the exponential distribution function, although it seems to underestimate the upper tail. From a visualisation point of view, the exponential distribution may be deemed appropriate.

To confirm the visual fit, an appropriate test statistic is used to evaluate the quality of the aggregate loss distribution.

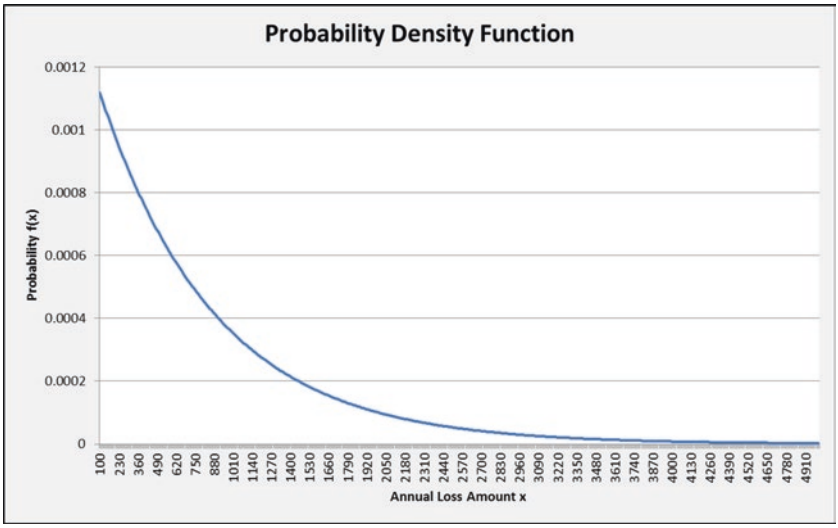

Fig. 15.10 Aggregate loss probability density function (Exponential distribution)

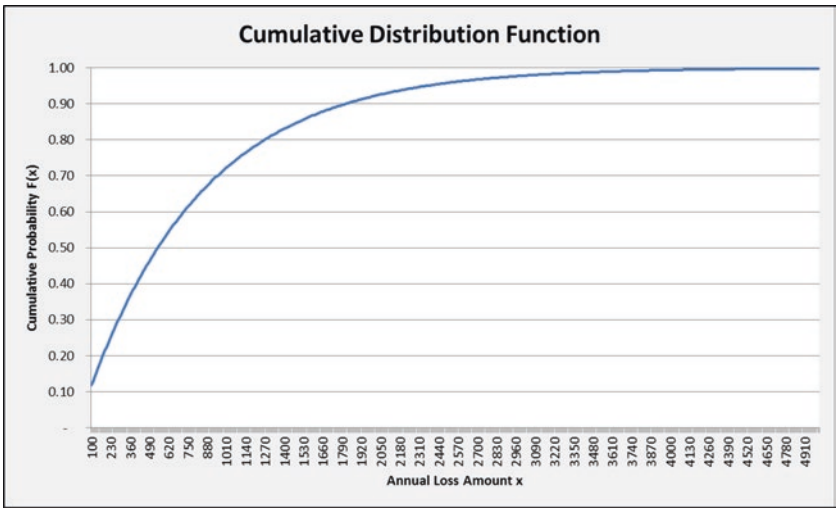

Fig. 15.11 Aggregate loss cumulative distribution function (Exponential distribution)

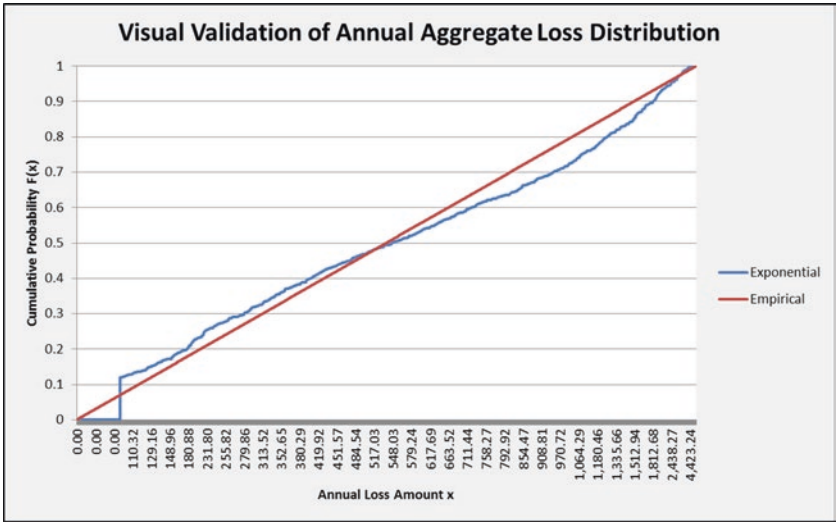

Fig. 15.12 Visualisation empirical versus fitted aggregate loss distribution function

The chi-squared test divides the observed annual aggregate losses into k intervals and compares the observed counts (number of data values observed in interval i) to the number expected given the fitted distribution (number of data values expected in interval i) (Packová and Brebera 2015, p. 18). To fulfill the minimum requirements in terms of fitted frequency,[4] the observed annual aggregate losses need to be associated to specific categories (Gray and Pitts 2012, pp. 63–65).

As for the exponential distribution, only one parameter is estimated in the fitting process and 36 categories are used during calculations, the appropriate chi-squared distribution has parameter $a = 34$ degrees of freedom. Applying the previously outlined formula, the calculation is rendered as follows:

$$X^2 = \sum \frac{(O - E)^2}{E} = 136.3417$$

This results in a p-value lower than 0.00001. As this value by far falls below the significance level of 0.05, the exponential distribution may not be deemed appropriate to reflect the aggregate loss distribution of the existing data set (GraphPad Software. 2019).

Furthermore, comparing the calculated X^2 value with the table value of the chi-squared distribution, that is between 18.493 for $a = 30$ degrees of freedom and 26.509 for $a = 40$ degrees of freedom for a confidence level of 95%, results in the conclusion that the null hypothesis is denied, as the calculated value is higher than the table value. Hence, it can be concluded that there is an extremely significant difference between the observed and expected values. This result is not surprising since the underlying claim size distribution also failed the goodness-of-fit test, but was still used for further processing in the Monte Carlo simulation because it still reflects parts appropriately.

To summarise, it can be observed empirically that the fit of the created distribution is not good; in particular, this distribution is not capable of reproducing the tail of the observed data. Formally, the hypothesis that the aggregate loss distribution has an exponential distribution is to be

[4] A cell is only deemed usable if the expected frequency is not too small, meaning all cells need to reach $E \geq 1$, and not more than 20% of the cells should have $E < 5$. If the frequencies are too low, neighbouring cells are combined.

denied. The conclusion is that this distribution does not provide an adequate description of the variation in the annual aggregate loss volumes that has been observed.

Although there seems to be no appropriate loss curve reflecting the severity and frequency for man-made fire/explosion disasters based on a historical data set, the developed loss curves (frequency—Poisson distribution/severity—one parameter Pareto distribution) may still be useful to the insurance industry. They can be integrated into the existing expert-based assessment processes for man-made disaster scenarios as they at least fit for specific sections and may support the estimation process from a quantitative/scientific perspective.

Conclusion

Due to the potential of man-made disasters to not only jeopardise an individual insurer's solvency position if the risk is not properly managed, but also to trigger market shocks and subsequent economic downturns, the need for a comprehensive approach to identify, assess, transfer, and mitigate the risk arises today even more than in the past. The objective of this research was to determine how the frequency and severity of such tail events can be evaluated and modelled based on empirical data. Due to the variety of triggers that require separate modelling approaches, this research was focused on man-made fire/explosion disasters since recent events, such as Tianjin harbor explosion, have shown the significance of this disaster type and their impact on the insurance industry and other markets.

In a broader perspective, it can be confirmed that the empirical modelling of man-made disaster scenarios remains very challenging since limited historical claims data exist (although different data sources were combined and a historical large fire/explosion loss database was developed) to model man-made catastrophes properly. For the time period 1974–2017, 114 large fire/explosion losses with a loss volume exceeding EUR 100 million were identified with an overall loss volume of EUR 36 billion. Based on the loss data, frequency, and severity, distributions were modelled on an individual basis and then combined through a Monte Carlo simulation to derive an aggregate loss distribution reflecting the industry loss data (collective risk model). For both, typical distribution types that are commonly used in the large/catastrophic loss modelling space were considered. In terms of the claim number, the Poisson distribution was fitted and a positive goodness-of-fit test was performed. In terms of the claim size, various

distributions—one parameter Pareto, Generalized Pareto, Weibull, and lognormal distribution were fitted, but for all of these distributions the goodness-of-fit test was negative. Thus, although an appropriate distribution for the claim number was identified, no proper distribution could be created in terms of claim size, which mainly refers to the significant standard deviation with regards to the loss volume.

Therefore, it is not surprising that the aggregate loss distribution, for which an exponential distribution was used, fails in the goodness-of-fit test as well. This result emphasises the challenges outlined at the beginning of this contribution and furthermore confirms that an assessment of man-made catastrophes is currently not possible if this is purely based on empirical modelling techniques by using historical loss data. Thus, the developed catastrophe loss curves should not be regarded as a stand-alone solution to the problem of quantifying tail events, but may be used as an additional tool for assessing man-made catastrophes since they provide an indication of the estimated loss potential. Accordingly, the quantitative outcome of this research should be integrated in the existing expert-based assessment approaches to ultimately create a more powerful and sophisticated methodology for evaluating man-made catastrophes. Since modelling approaches evolve, especially in times of predictive analytics, research on modelling man-made disasters should be continued and alternative approaches should be further explored.

References

ATEX Explosion Hazards Ltd. (2018). *List of historic explosions (Dust, vapour and gas)*. Source. Retrieved January 5, 2019, from http://www.explosionhazards.co.uk/list-of-historic-explosions/.

Banks, E. (2009). *Risk and financial catastrophe*. Hampshire: Palgrave Macmillan.

Brüske, S., Cottin, C., Hiebing, A., & Hille, B. (2010). Die stochastische Modellierung von Großschäden für den Einsatz in internen Risikomodellen der Schadenversicherung. *ZVersWiss, 99*(2), 133–154.

Cambridge Centre for Risk Studies (2018, March). *Impact of severe Natural Catastrophes on Financial Markets.*

Clark, K., Chang, H., & Manghnani, V., (2015). Chapter 5 – Catastrophe risk. In IAA/AAI (Ed.), *IAA risk book: Governance, regulation and management of insurance operations*. n.p. n.p.

Cottin, C., & Döhler, S. (2013). *Risikoanalyse: Modellierung, Beurteilung und Management von Risiken mit Praxisbeispielen*. Wiesbaden: Springer Verlag.

Cutler, D. (2013). *Factbox: Industrial accidents in the last two decades*. Retrieved January 5, 2019, from https://www.reuters.com/article/us-usa-explosion-texas-accidents/factbox-industrial-accidents-in-the-last-two-decades-idUSBRE93H1EM20130418.

Embrechts, P., & Schmidli, H. (1994). Modelling of extremal events in insurance and finance. *Zeitschrift für Operations Research, 39*(1), 1–34.

Embrechts, P., Klüppelberg, C., & Mikosch, T. (2003). *Modelling extremal events for insurance and finance*. Berlin and Heidelberg: Springer Verlag.

Forbes, C., Evans, M., Hastings, N., & Peacock, B. (2011). *Statistical distributions*. New Jersey: John Wiley & Sons.

Gondring, H. (2015). *Versicherungswirtschaft: Handbuch für Studium und Praxis*. München: Franz Vahlen Verlag.

GraphPad Software (2019). *P value calculator*. Retrieved February 3, 2019, from https://www.graphpad.com/quickcalcs/pvalue1.cfm.

Gray, R., & Pitts, S. (2012). *Risk modelling in general insurance: From principles to practice*. Cambridge: Cambridge University Press.

Hosking, J., & Wallis, J. (1987). Parameter and Quantile estimation for the generalized Pareto distribution. *Technometrics, 29*(3), 339–349.

Lloyd's. (2018). *Realistic disaster scenarios: Scenario specification*. Retrieved January 3, 2019, from https://www.lloyds.com/market-resources/underwriting/realistic-disaster-scenarios-rds.

Marsh. (2012). *Marsh insights: Property*. Retrieved January 10, 2019, from https://www.marsh.com/content/dam/marsh/Documents/PDF/US-en/Marsh-Insights-Property-Fall-2012.pdf.

Marsh. (2014). *Historical loss experiences in the global power industry*. Retrieved January 5, 2019, from http://www.oliverwyman.com/content/dam/marsh/Documents/PDF/UK-en/Historical%20Loss%20Experiences%20in%20the%20Global%20Power%20Industry-08-2014.pdf.

Marsh. (2016). *The 100 largest losses 1974–2015: Large property damage losses in the hydrocarbon industry – 24th edition*. Retrieved December 28, 2018, from https://www.marsh.com/content/dam/marsh/Documents/PDF/UK-en/100%20largest%20losses%201974%20to%202015-03-2016.pdf.

Marsh. (2018). *The 100 largest losses 1978–2017: Large property damage losses in the hydrocarbon industry – 25th edition*. Retrieved December 28, 2018, from https://www.marsh.com/content/dam/marsh/Documents/PDF/UK-en/100-largest-losses.pdf.

Mikosch, T. (2009). *Non-life insurance mathematics: An introduction with the Poisson Process*. Berlin and Heidelberg: Springer Verlag.

Mitchell-Wallace, K., Foote, M., Hilier, J., & Jones, M. (2017). *Natural catastrophe risk management and modelling: A practitioner's guide*. Chichester: John Wiley & Sons.

Nwobi, F., & Ugomma, C. (2014). A comparison of methods for the estimation of weibull distribution parameters. *Metodološki zvezki, 11*(1), 65–78.

OECD. (2019). *Inflation*. Retrieved January 21, 2019, from https://data.oecd.org/price/inflation-cpi.htm.

Packová, V., & Brebera, D. (2015). *Loss distributions in insurance risk management*. Retrieved January 21, 2019, from http://www.inase.org/library/2015/barcelona/bypaper/ECBAS/ECBAS-03.pdf.

Peng, L., & Welsh, A. (2001). Robust estimation of the generalized Pareto distribution. *Extremes, 4*(1), 54–65.

Pobočíková, I., & Sedliačková, Z. (2014). Comparison of four methods for estimating the Weibull distribution parameters. *Applied Mathematical Sciences, 8*(83), 4137–4149.

Singh, V., & Guo, H. (1995). Parameter estimation for 3-parameter generalized pareto distribution by the principle of maximum entropy (POME). *Hydrological Sciences Journal, 40*(2), 165–181.

Swiss Re (2016). *Analysis of Tianjin port explosion: Risk management is the key*. Retrieved August 17, 2019, from https://www.swissre.com/china/Analysis_of_Tianjin_Port_Explosion.html.

Swiss Re Institute (2018a). Information and methodology of sigma explorer data. Retrieved December 28, 2018, from http://www.sigma-explorer.com/documentation/Methodology_sigma-explorer.com.pdf.

Swiss Re Institute. (2018b). *sigma 1/2018: Natural catastrophes and man-made disasters in 2017: A year of record-breaking losses*. Retrieved January 15, 2019, from http://institute.swissre.com/research/overview/sigma/1_2018.html#tab_2.

Swiss Re Institute. (2018c). *Natural catastrophes and man-made disasters in 2017: A year of record-breaking losses*. Retrieved January 3, 2019, from http://media.swissre.com/documents/sigma1_2018_en.pdf.

The World Bank Group. (2019). *Consumer price index (2010 = 100)*. Retrieved January 28, 2019, from https://data.worldbank.org/indicator/FP.CPI.TOTL.

Thornton, R. (2016). *Man-made catastrophes: A perpetual emerging risk*. Retrieved January 28, 2019, from https://www.globalreinsurance.com/man-made-catastrophes-a-perpetual-emerging-risk/1419434.article.

Wälder, K., & Wälder, O. (2017). *Methoden zur Risikomodellierung und des Risikomanagements*. Wiesbaden: Springer Verlag.

Zaiontz, C. (2019). *Fitting Weibull parameters using MLE and Newton's method*. Retrieved January 17, 2019, from http://www.real-statistics.com/distribution-fitting/distribution-fitting-via-maximum-likelihood/fitting-weibull-parameters-mle-newtons-method/.

Zea Bermudez, P., & Kotz, S. (2010). Parameter estimation of the generalized Pareto distribution – Part I. *Journal of Statistical Planning and Inference, 140*(6), 1353–1373.

Zurich Insurance Group. (2017). *Assessing man-made catastrophes*. Retrieved December 3, 2018, from https://www.zurich.com/en/knowledge/articles/2017/03/assessing-man-made-catastrophes.